Experimental & Analytical Flexural Behavior of Concrete Beams Reinforced with Basalt Fiber Reinforced Polymers Bars

Abeer M. Erfan[a*], Yasser A. Algash[b], Taha A. El-Sayed[c]
[a,c] Structural Engineering Department, Faculty of Engineering at Shoubra, Benha University, 108 Shoubra St., Shoubra, Cairo, Egypt
[b] Aviation and Engineering Technology Institute, Structural Engineering Department, Cairo, Egypt

Abstract

This research offers an experimental and analytical investigation the behavior of RC beams under bending reinforced with BFRP bars. BFRP bars has a fewer stiffness than reinforced steel, that would be considered for the cases of ultimate and serviceability. A ten RC beams of 150mm wide, 250mm height and 2100mm length, were tested to failure under bending. A non-linear analysis (NLA) using ANSYS V. 14.5 was created to represent the tested beams performance. It can be reflected an acceptable agreement between did results that were made experimentally and analytically. BFRP bars in this study showed improving ductility of beams and reduced the unwanted brittle failure of beams. The performances of the above beams were compared with the controlled specimen and the results are presented in this paper.

Keywords: Concrete beams, BFRP bars, Deflection, Crack pattern, Load Vs Deflection, non-linear analysis (NLA), ANSYS V.14.5.

1. Introduction

BFRP bars are the most recent sort of FRP reinforcement used in structural engineering. The mechanical characteristics of BFRP bars are similar to those of GFRP [2-4], so it can be supposed that basalt and glass RC members can be reflected according to the similar design principles [1]. However, BFRP is a reasonably new technique, so performance of BFRP RC elements has to quiet be methodically observed.

Compared with steel reinforcement, the BFRP has higher tensile strength, higher corrosion resistance, lower density, higher fatigue resistance, better insulation and some other virtues. Apparently, if the BFRP is used as alternative for steel reinforcement, steel bars corrosion can be avoided thoroughly. Peak stiffness and strength upon weight of BFRP gave an interesting

another to the traditional strengthening and repair resources.

*Corresponding author:

Email: abir.arfan@feng.bu.edu.eg

Additionally, basalt fiber is a relative new arrival to FRP [5-6]. At present, numerous research studies have been performed on carbon fiber and glass fiber reinforced concrete [7], while studies on concrete slabs reinforced with BFRP are limited.

The targets of this paper are, first of all, to manufacture BFRP bars by means of obtainable stuff in the local shop, furthermore, to display experimental results of BFRP beams in expression of the deflection, cracking, and ultimate failure loading capacity. So, for this purpose, ten beams have been tested under bending as following.

2. Experimental Study

The beams samples were examined under 2000kN universal testing machine with 1800mm length as in Fig. 1. The aim of this study was getting the ultimate failure load, ultimate midspan deflection, and failure mode for control beams, to associate their behavior with BFRP beams.

2.1. Material used

1. Fine aggregate: was of natural siliceous sand. The fineness modulus and specific gravity was found to be 2.64 and 2.74 [9].
2. Coarse aggregate: was crushed stone aggregate with a specific gravity 2.89 [9].
3. Cement: Ordinary Portland type CEM I 42.5 N with a specific gravity 3.15 [9].
4. Silica Fume: with a specific gravity 2.30 and normal range from 5 to 20% of cement weight.
5. Tapped Water: for mixing and curing procedures [9].
6. Super plasticizer: with a density of 1.2kg/litre [9].
7. Reinforcing steel: Two types of reinforcing steel: Type I: Normal mild steel 24/35 (plain bars) of diameter 6 mm, Type II: High grade steel 36/52 (deformed bars) of diameter 10 and 12 mm [9].
8. Basalt fiber reinforced polymers (BFRP) bars; see Table 1 & Fig. 1.

Table 1: BFRP properties

Property	Measured Value
Density (MPa)	2.68
Tensile Strength, *f*u (MPa)	1400
Tensile Modulus (Gpa)	56
Ultimate Strain, €u (%)	24

Fig. 1. Ribbed & smooth BFRP bars.

2.2. Mortar mix design

The mix design of concrete was prepared to achieve 30MPa & 60MPa compressive strengths (f_{cu}) of at 28days. Properties of mix are summarized in below Table 2.

Table 2: Mix design of concrete

Item	Cement (kg/m^3)	Coarse aggregate (kg/m^3)	Fine aggregate (kg/m^3)	Water (kg/m^3)	Silica Fume (kg/m^3)	Super plasticizer (kg/m^3)
Per m^3 of concrete (30MPa)	350	1280	640	175	---	3.5
Per m^3 of concrete (60MPa)	600	1100	550	140	60	16

2.3. Specimens characterization

The experimental work contains ten RC beams with dimensions of 150 mm x 250 mm in wide, depth and 2100 mm at length were examined till failure. All tested beams were reinforced with basalt bars except for the control ones reinforced using steel bars also, all beams examined using 2000kN capacity testing machine. Dimension of concrete and reinforcement specifics for all specimens as in in Fig. 2. Summarization of beam specimens as in below Table 3.

Table 3: Specimens record

Series	Specimen Designation	Details of Reinforcement			The reinforcement steel ratio μ (%)
		Tension	Compression	Stirrups	
Group I	BS30 (Control)	2 φ14	2 φ 8	φ8@100	1.03
	B30-1	2 φ 8	2 φ 8	φ8@150	0.33
	B30-2	2 φ10	2 φ 8	φ8@100	0.52
	B30-3	2 φ14	2 φ 8	φ8@80	1.03
	B30-4	2 φ18	2 φ 8	φ8@50	1.60
Group II	BS60 (Control)	2 φ14	2 φ 8	φ8@100	1.03
	B60-1	2 φ 8	2 φ 8	φ8@150	0.33
	B60-2	2 φ10	2 φ 8	φ8@100	0.52
	B60-3	2 φ14	2 φ 8	φ 8@80	1.03
	B60-4	2 φ18	2 φ 8	φ8@50	1.6

2.4. Test framework

All specimens were examined under 2000kN capacity bending machine for operative span of 1800mm as shown in Fig. 3. Midspan deflections was measured using LVDT 20kN load increments. Ultimate failure load and midspan deflection correlation were logged by a system of data acquisition. Also, crack configuration was noted.

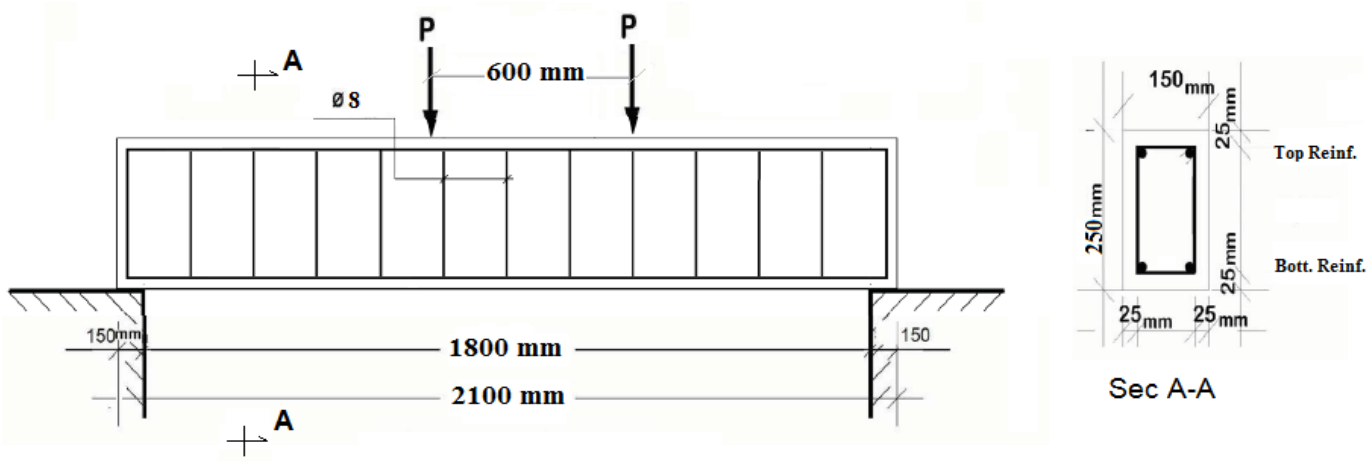

Fig. 2: Typical specimen's dimesions and details of reinforcement

Fig. 3: Test framework representation

3. Results and Discussion

Through the experimental test, the tested beams were naked detected until first crack occurs till failure. First crack corresponding load was recorded and the midspan deflection at first crack also recorded. Table 3 presented the obtained results for all tested beams. The mean value of initial cracking load was 16.4KN and 18.0KN for first and second testing groups of beams corresponding to an average deflection at first crack load of 1.78mm and 2.14mm for first and second group respectively. El-Nemr [10], concluded similar ratios in their results in using glass fibers bars. After reaching the extreme load, sudden drop in the experimental load occurs indicting to failure. This sudden failure may be due to the mechanism of failure for concrete

sections reinforced using FRP bars.

3.1. Failure mode

The failure mode for the tested reinforced concrete beams were observed by naked eyes. This mode of failure was varied between flexural failures especially for beams reinforced using steel bars of BS30 and BS60. For specimens B30- 1 to B30- 3 and B60- 1 to B60- 3, the failure was tension failure but in basalt bars and it occurs suddenly which refer to the failure mechanism of fiber bars so, it is B.F basalt bars failure. El-Nemr [7], recorded similar mode of failure in specimens reinforced by FRP bars. Table 3 represent this mode of failure, while the failure mode of beams B30- 4 and B60- 4 was compression failure. The concrete crushing occurs in the over reinforced basalt bars specimens. Although this compression failure the tension cracks occurs until the concrete crushed.

3.2. Patterns of crack and width

First cracks occurred in all specimens approximately in the tension zone at the middle of the beams. The other cracks occurred as tension cracks as shown in Fig. 4 for all specimens showing tension failure for beam B30- 1 to B30- 3 and B60- 1 to B60- 3 with different of its failure load but there was a sudden crushing in basalt bars due to its failure mechanism after tension cracks in concrete occurred. For specimens B30- 4 and B60- 4 the cracks occurred in tension zone at the beginning of the loading but due to the increasing in reinforcement ratio, the concrete crushed at compression zone causing the beam failure as shown in Figs. 5 & 6.

For the cracks width of different concrete beams were measured using optical micrometer. The initial crack width was measured with micrometer to record 0.5mm, 0.4mm, 0.3mm, 0.1mm and 0.1mm for BS30, B30- 1, B30 -2, B30- 3 and B30- 4 respectively, which represent the first group of concrete strength 30 MPa. For the second group of concrete strength 60 MPa, its notice that the initial crack width decrease due to increase in concrete strength. The initial cracks width was 0.3mm, 0.2mm, 0.15mm, 0.1mm and 0.05mm for BS60, B60- 1, B60- 2, B60- 3 and B60- 4 respectively.

At the final stages of loading which leads to failure, the cracks increased in numbers and width to lead to failure. The concrete strength and the reinforcement ratio have the key parameter to decrease the width of cracks for group 2 compared to group 1. The crack widths were 3.5mm, 3.1mm, 2.5mm, 2.1mm and 1.9mm for BS30, B30- 1, B30- 2, B30- 3 and B30- 4 respectively. For the second group, its notice that the concrete strength has the main effect in decreasing the cracks width at failure as shown in Fig. 6. The cracks after failure of this group were 3.2mm,

2.9mm, 2.1mm, 1.8mm and 1.5mm for BS60, B60- 1, B60- 2, B60- 3 and B60- 4 respectively.

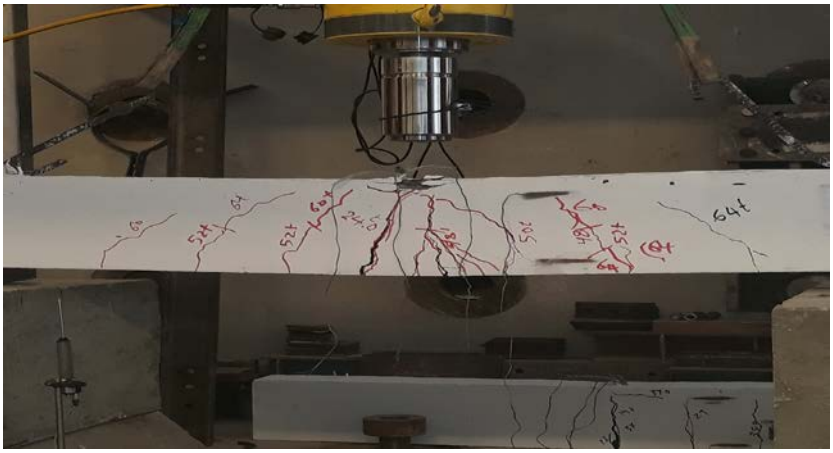

Fig.4: Typical Experimental Crack pattern for beams

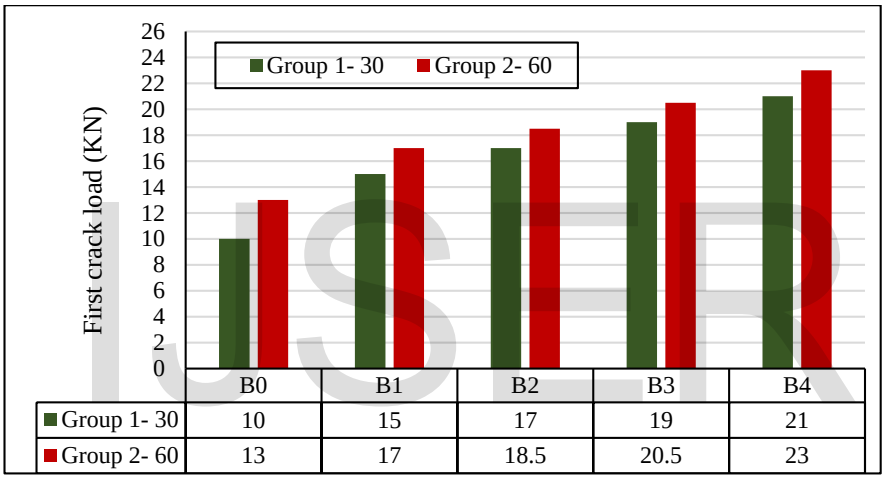

	B0	B1	B2	B3	B4
Group 1- 30	10	15	17	19	21
Group 2- 60	13	17	18.5	20.5	23

Fig. 5: Comparison between first crack loads for tested beams

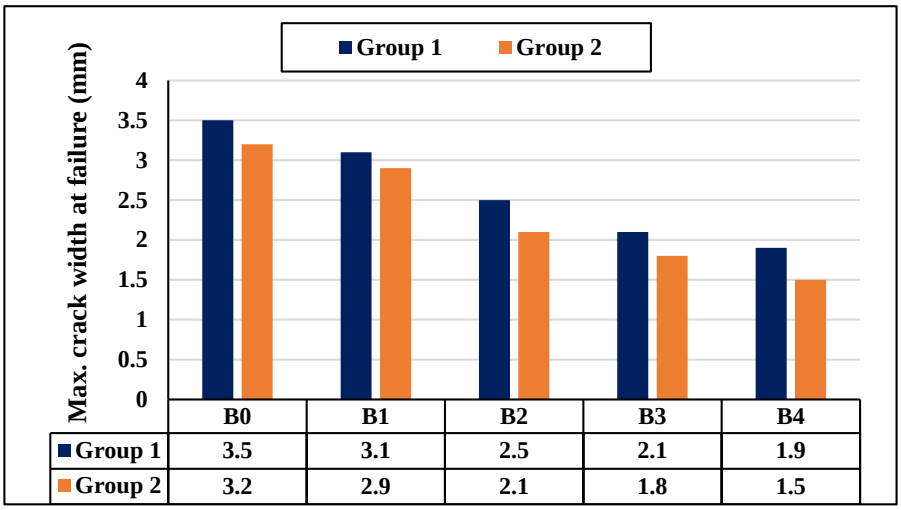

	B0	B1	B2	B3	B4
Group 1	3.5	3.1	2.5	2.1	1.9
Group 2	3.2	2.9	2.1	1.8	1.5

Fig. 6: Comparison between maximum crack widths for tested beams

Table 4: Experimental Mode of failure

Series	Specimen Designation	The reinforcement steel ratio (%)	Mode of failure	Experimental Failure load (KN)
Group I	BS30 (Control)	1.03	T.F	37.0
	B30-1	0.33	B.F	75.0
	B30-2	0.52	B.F	111.0
	B30-3	1.03	B.F	130.0
	B30-4	1.60	C.F	150.0
Group II	BS60 (Control)	1.03	T.F	45.0
	B60-1	0.33	B.F	90.0
	B60-2	0.52	B.F	140
	B60-3	1.03	B.F	160
	B60-4	1.6	C.F	190

- T.F: tension failure in steel bars, B.F: basalt bars failure, C.F: compression failure in concrete

3.3 Ultimate failure load - deflection

The experimental failure loads for the two beams groups and its corresponding deflections were recorded in Table 5 and Figs. 7 & 8. The deflection was recorded using LVDT at the mid span verse to the corresponding experimental loads. It was observed that the load-deflection curves for specimens reinforced using basalt bars was semi bilinear especially after reaching failure load, it decreases very rabidly. This behavior due to the failure mechanism of basalt bars and the type of concrete. For the first group which has concrete strength equals to 30MPa, the failure loads were 37.0KN for the control specimen which reinforced by steel bars verse to deflection of 31.0mm. when using the basalt bars, the deflection decrease and the failure load increase due to high tensile strength of basalt bars. The failure loads were 75.0KN, 111.0KN, 130.0KN and 150KN verse to deflection of 25.0mm, 22.0mm, 19.0 mm and 15.0 mm for B30-1, B30- 2, B30- 3 and B30- 4 respectively.

For the group of concrete strength of 60.0 MPa, the failure load of BS60 was 45.0 KN which increase with approximately 22.0% compared to BS30. Also, the deflection recorded 37.2 mm due to increase in failure load. For the specimens reinforced using the basalt bars with different ratio recorded an increase in failure load of 20.0%, 26.0%, 23.0% and 27.0% for B60- 1, B60-2, B60- 3 and B60- 4 respectively verse to deflection of 30.0mm, 27.7mm, 23.3mm and 19.1mm as in Table 5. This behavior of increasing in failure load was due to the effect of concrete strength and the tensile strength of basalt bars. These results are accompanied with Jason Duic. et.al [8].

Table 5: Results of Experimental study

Series	Specimen Designation	First crack load, kN	Ultimate failure load, kN	Deflection at first crack load, mm	Deflection at ultimate load, mm	Ductility index (%)
Group I	BS30 (Control)	10.0	37.0	2.0	31.0	6.5
	B30-1	15.0	75.0	1.9	25.0	7.6
	B30-2	17.0	111.0	1.8	22.0	8.2
	B30-3	19.0	130.0	1.7	19.0	8.9
	B30-4	21.0	150.0	1.5	15.0	10.0
Group II	BS60 (Control)	13.0	45.0	4.5	37.2	12.1
	B60-1	17.0	90.0	1.9	30.0	6.3
	B60-2	18.5	140	1.7	27.7	6.1
	B60-3	20.5	160	1.4	23.3	6.0
	B60-4	23.0	190	1.2	19.1	6.2

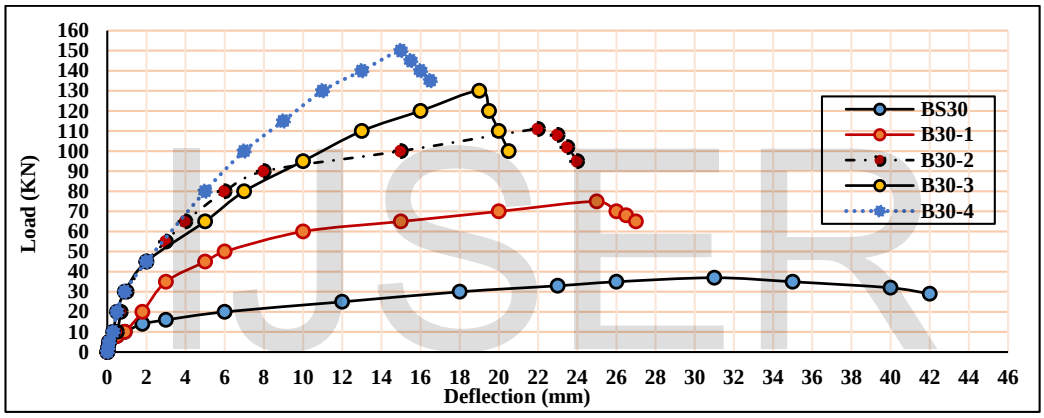

Fig. 7: Load deflection curve for the first group

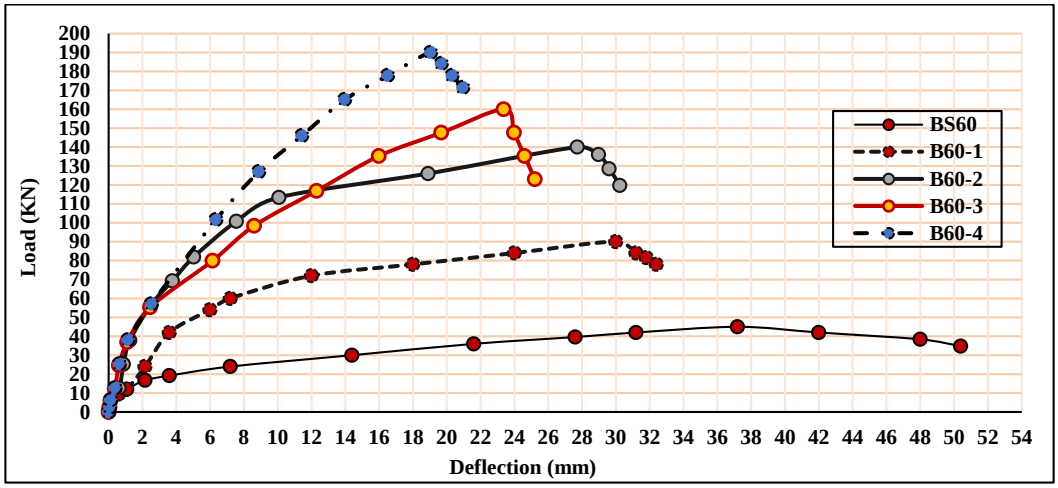

Fig. 8: Load deflection curve for the second group

3.4 Ductility responses

The ductility represents the behavior of the specimens due to existing of steel or FRP

reinforcement. The difference between steel and FRP reinforcement is that steel exhibit yielding to large amount of ductility but FRP not exhibit the same behavior. The ductility obtained from specimens reinforced using basalt bars related to the high experimental failure load to the load of the first crack.

Fig. 9 and Table 5 show a comparison between the obtained ductility for each specimens. For the group of concrete strength of 30.0 MPa, the ductility ratio was 6.5 % to 10.0 %. For specimens of the second group, the ductility was varying between 6.0 % to 12.0 %.

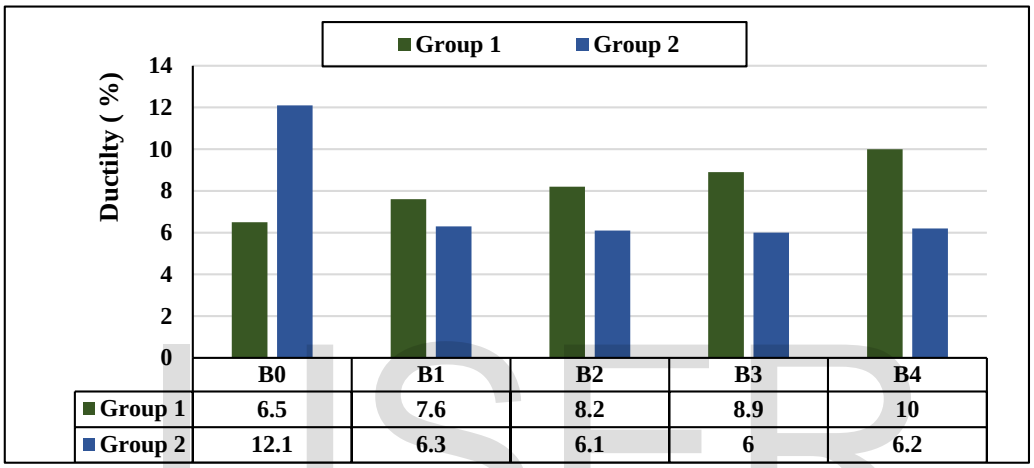

	B0	B1	B2	B3	B4
Group 1	6.5	7.6	8.2	8.9	10
Group 2	12.1	6.3	6.1	6	6.2

Fig. 9: Comparison between ductility ratios of tested beams

4. Non-Linear analysis (NLA)

NLA was done to verify the BFRP beams with experimental results. The ANSYS software [10] was used to verify this purpose. The failure load, deflection, first cracks, total cracks and ductility are the main parameters which will discussed in the finite element program. Therefore, an agreement and correlation between the obtained NLFEA results and the experimental ones which verify the model of ANSYS. The program for the beams which used in experimental test is the same for what in NLFEA.

Element solid65 is used for representing concrete beams and Link64 spare was used to represent the reinforcing bars for steel and basalt bars as shown in Fig.10.

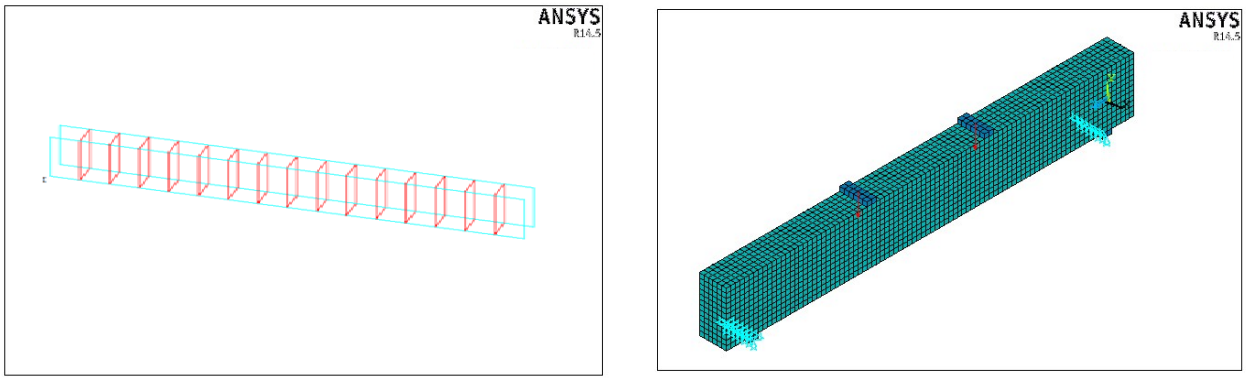

(a) (b)

Fig.10: Analytical Model, a) link 64 for reinforcing bars , b) solid 65 for concrete.

4.1 Analytical ultimate failure load

The analytical failure loads for the examined beams and its corresponding deflections were recorded in Table 6. The deflection was recorded using the obtained results from ANSYS results at the mid span verse to the corresponding experimental loads. It was observed that the load-deflection curves for specimens reinforced using basalt bars was agreed with the behavior of experimental results. For the group which has concrete strength equals to 30MPa, the failure loads were 30.0KN for the control specimen of concrete strength of 30 MPa. For specimens B30- 1, B30- 2, B30- 3 and B30- 4, the failure loads were 64.0KN, 100.0KN, 108.0KN and 131.0KN respectively. It's observed the increase in failure load for beams reinforced using basalt bars accompanied with experimental results.

For the beams which has concrete strength of 60MPa, the obtained results from NLFEA was as shown in Table 6. For BS60 the failure load was 36.0KN but the failure loads were 76.5KN, 126.0KN, 132.8KN and 165.5KN for B60- 1, B60- 2, B60- 3 and B60- 4 respectively. This increase in failure loads for the specimens reinforced using basalt bars is due to the high tensile strength of basalt bars with respect to the steel bars. Also, the basalt failure mechanism which effect in the mode of failure.

Table 6: Results of analytical NLA

Series	Specimen Designation	First crack load, KN	Ultimate failure load,	Deflection at first crack load,	Deflection at ultimate load,	Ductility index

			KN	mm	mm	(%)
Group I	BS30 (Control)	7.0	30.0	1.5	24.8	23.3
	B30-1	7.0	64.0	0.9	21.5	10.9
	B30-2	7.0	100.0	0.8	19.8	7.0
	B30-3	7.0	108.0	0.6	16.5	6.4
	B30-4	7.0	131.0	0.5	13.0	5.3
Group II	BS60 (Control)	10.5	36.0	1.5	29.7	29.2
	B60-1	10.5	76.5	0.5	25.5	13.7
	B60-2	10.5	126.0	0.5	24.9	8.3
	B60-3	10.5	132.8	0.3	19.35	7.9
	B60-4	10.5	165.5	0.4	16.5	6.3
	average	8.75	96.98	0.75	21.16	11.83

4.2 Ultimate midspan deflection

The deflection of the specimens which simulated in NLA was recorded to compare with experimental deflection obtained. The obtained results were presented in Table 6. The deflections for first group were 24.8mm, 21.5mm, 19.8mm, 16.5mm and 13.0mm for BS30, B30- 1, B30- 2, B30- 3 and B30- 4 respectively. It was observed in Table 6 that the deflection for the second group was greater than the first group although it had compression strength 60.0 MPa. This is due to the failure loads of this specimens but at the same load the deflection is less than it. While the deflection recorded 37.2mm, 30.0mm, 27.7mm, 23.3mm and 19.1mm for BS60, B60- 1, B60- 2, B60- 3 and B60- 4 respectively with an average of 27.5mm.

Table 7: Experimental and NLA Analysis comparison

Series	Specimen Designation	Ultimate Failure load, Pult KN		Deflection at ultimate load, Δult mm		Pult NLA / Pult Exp.	Δult NLA / Δult Exp.
		NLA	EXP.	NLA	EXP.		
Group I	BS30- Control	30.0	37.0	24.8	31.0	0.80	0.80
	B30-1	64.0	75.0	21.5	25.0	0.85	0.86
	B30-2	100.0	111.0	19.8	22.0	0.90	0.90
	B30-3	108.0	130.0	16.5	19.0	0.83	0.86
	B30-4	131.0	150.0	13.0	15.0	0.87	0.86

Group II	BS60-Control	36.0	45.0	29.7	37.2	0.8	0.79
	B60- 1	76.5	90.0	25.5	30.0	0.85	0.85
	B60-2	126.0	140	24.9	27.7	0.9	0.89
	B60-3	132.8	160	19.35	23.3	0.83	0.83
	B60-4	165.5	190	16.5	19.1	0.87	0.86
Average		96.9	112.8	21.2	24.9	0.85	0.86

.

5. Comparison between experimental results and NLA

After obtained all available results from non-linear finite element analysis, a comparison between the experimental results and NLA results.

5.1 Ultimate load

Acceptable agreement between the experimental and NLA failure load as showed in Table 7 and Fig. 11. It was found that Pu NLA/Pu exp. with a ratio of 0.80 for control in the first group but it was 0.85 in the second group which showed good agreement between the two obtained results. For beams B30- 1, B30- 2 and B30- 3 and B30- 4 the ratios of Pu NLFEA/Pu exp. were 0.85, 0.83, 0.87 and 0.80 respectively. For beams B60- 1, B60- 2 and B60- 3 and B60- 4 Pu NLA/Pu exp. ratios were 0.90, 0.83, 0.87 and 0.85 respectively. The NLA displayed good correspondence with experimental results.

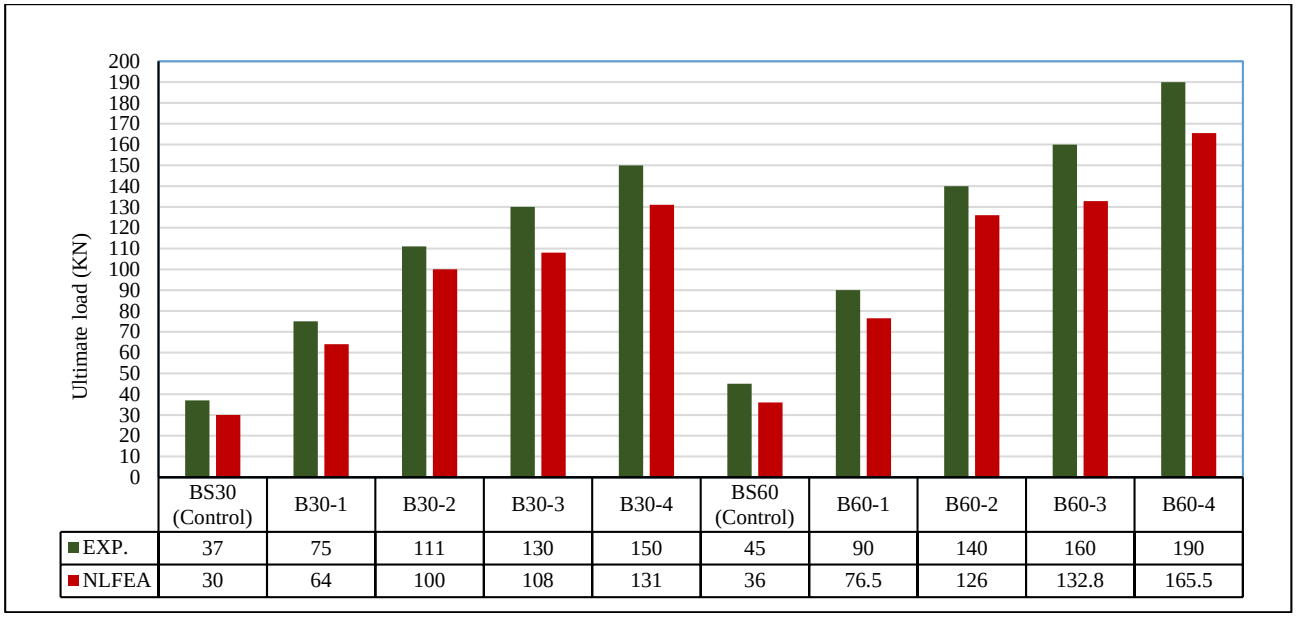

	BS30 (Control)	B30-1	B30-2	B30-3	B30-4	BS60 (Control)	B60-1	B60-2	B60-3	B60-4
EXP.	37	75	111	130	150	45	90	140	160	190
NLFEA	30	64	100	108	131	36	76.5	126	132.8	165.5

Fig. 11: Experimental and analytical ultimate loads comparasions

5.2. Ultimate midspan deflection

Figs. 12 &13 and Table 7 displayed comparison between midspan deflection between experimental and NLA. Fig. 12 showed the harmonizing between the two obtained results. For the deflection of beams B30- 1, B30- 2 and B30- 3 and B30- 4 the ratios of Δult NLFEA/Δult exp. were 0.86, 0.90, 0.86 and 0.86 respectively. For beams B60-1, B60- 2 and B60- 3 and B60-4 Δult NLA/Δult exp ratios were 0.89, 0.83, 0.86 and 0.86 respectively showing good agreement. Fig. (13 a,b) showed comparisons between experimental and NLA load deflection curves for all tested specimens. As a result of previous, the analytical models provided a satisfactory load deflection response.

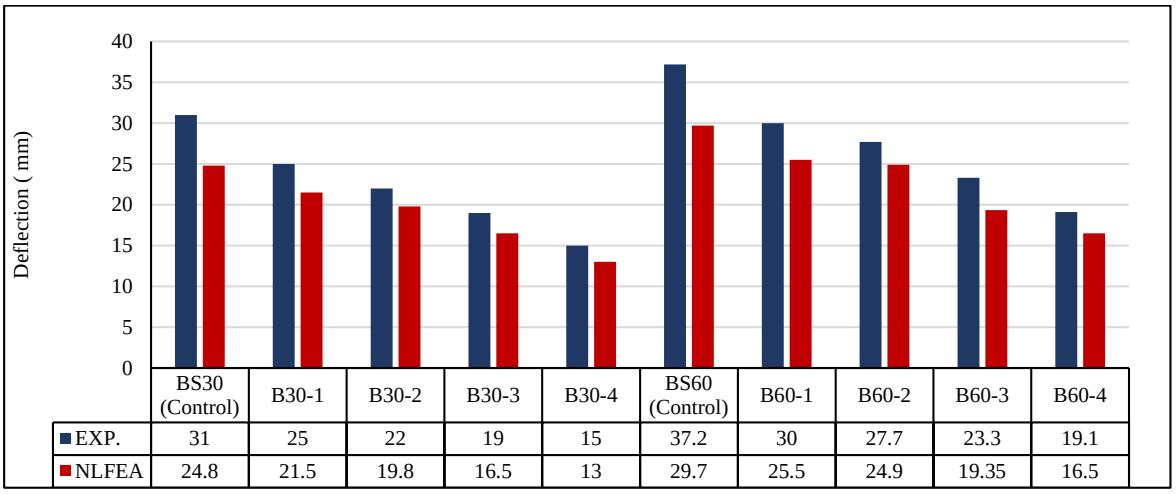

	BS30 (Control)	B30-1	B30-2	B30-3	B30-4	BS60 (Control)	B60-1	B60-2	B60-3	B60-4
EXP.	31	25	22	19	15	37.2	30	27.7	23.3	19.1
NLFEA	24.8	21.5	19.8	16.5	13	29.7	25.5	24.9	19.35	16.5

Fig. 12: Experimental and analytical midspan deflection comparisons.

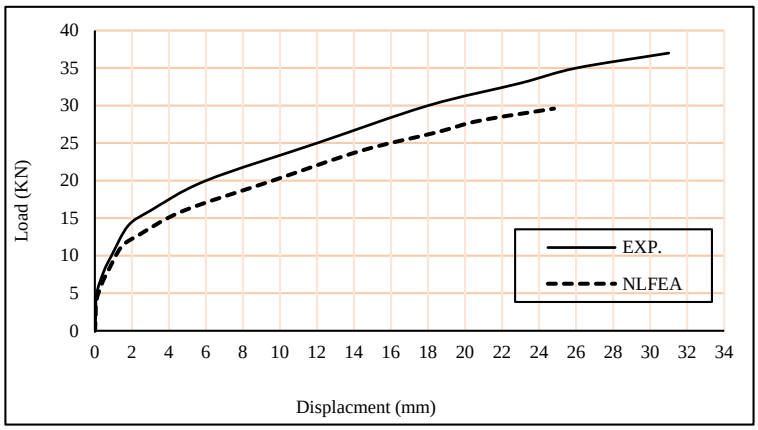

a) BS30

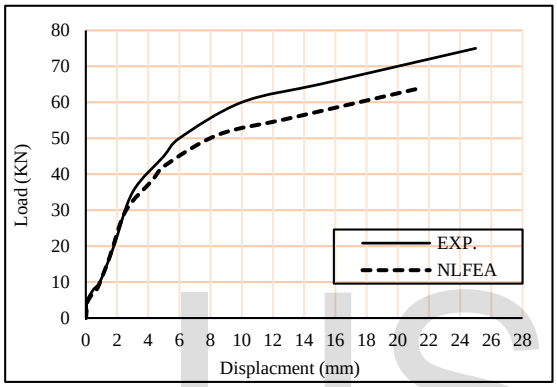

(b)B30- 1

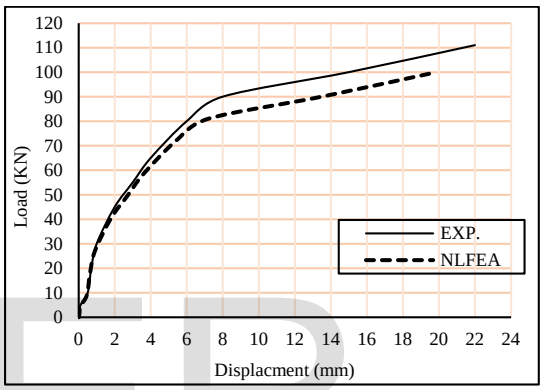

C) B30- 2

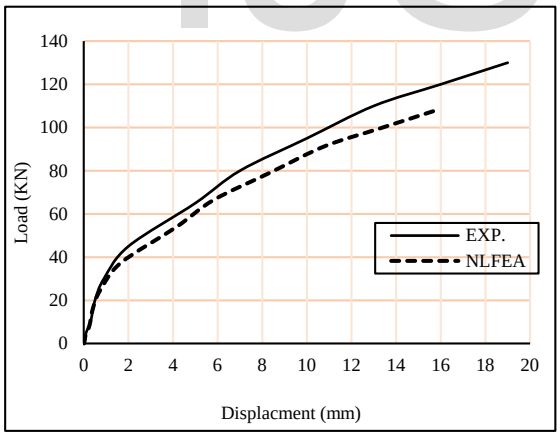

d)B30- 3

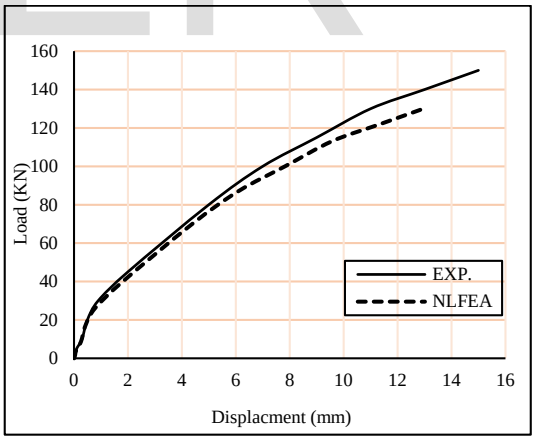

e) B30- 4

Fig. 13-a: Group 1, experimental and analytical load-deflection curves comparasions

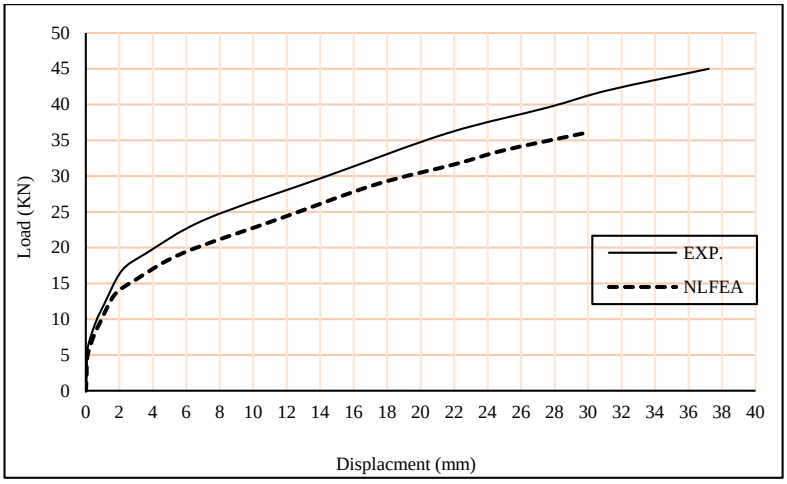

a) BS60

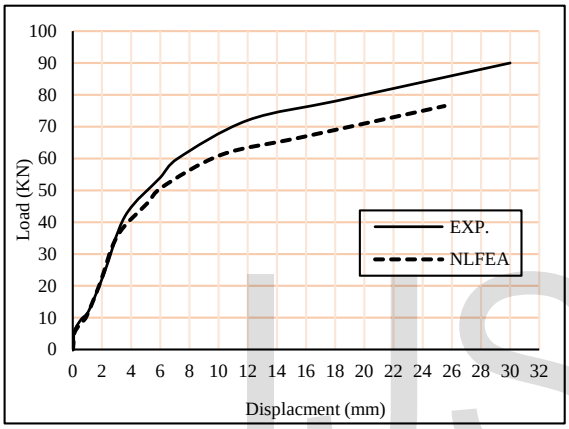

b)B60- 1

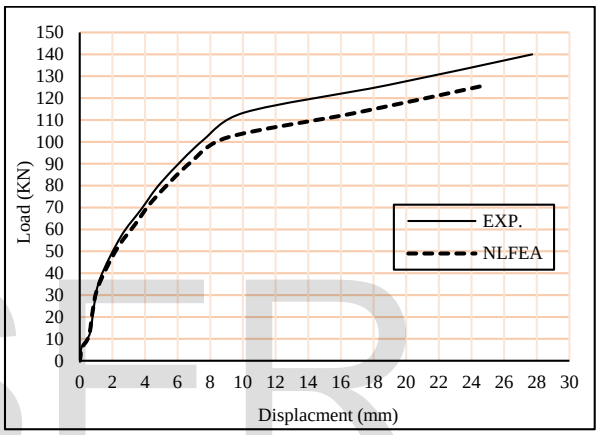

c) B60- 2

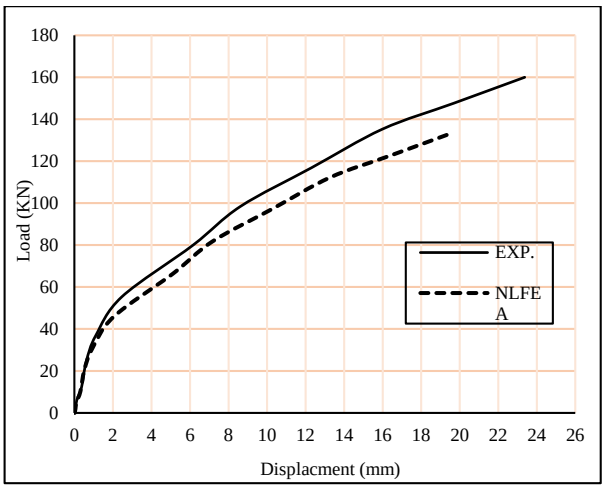

d) B60- 3

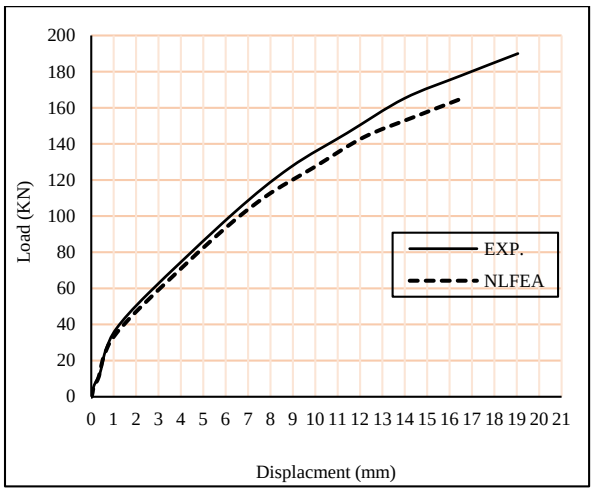

e) B60- 4

Fig. 13-b: Group 2, experimental and analytical load-deflection curves comparasions

5.3. Pattern of cracks

Pattern of cracks got from experimental work and NLA for all beams presented an approximately similar patterns of crack propagation in flexural failure. Fig.14 specify a

comparison between those got. These cracks started at the middle of the beams and grow into diagonal and grew toward the points of loading. After that it increase in length and width till failure.

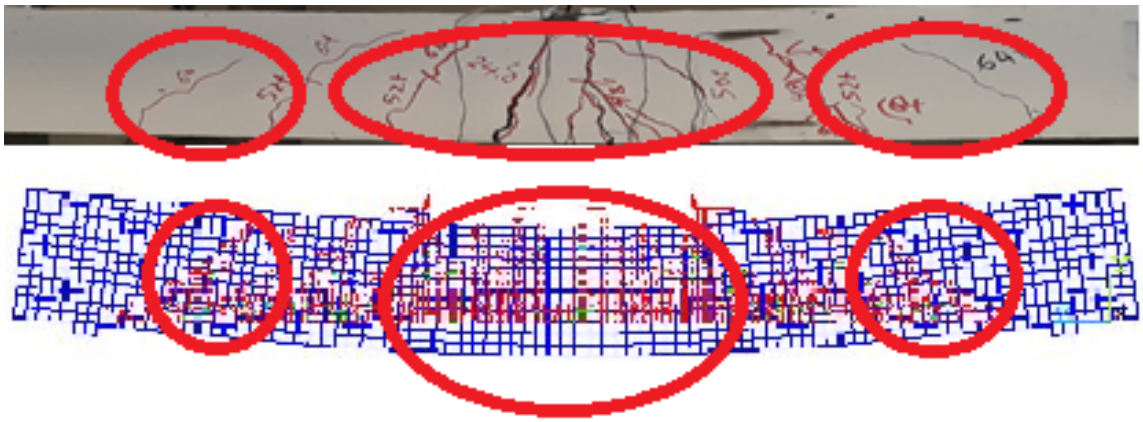

a)

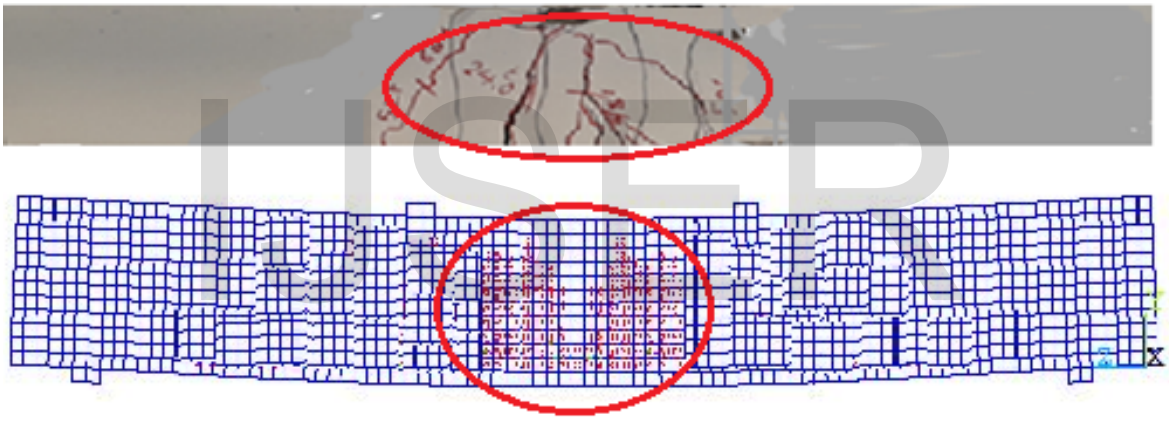

b)

Fig.14: Pattern of cracks for examined beams; a) Control brams; b) BFRP beams

6. Conflict of Interest: No conflict of Interest.

7. Conclusion

From the previous work, the following conclusions were drawn:

1- The BFRP bars showed mechanical failure mechanism as FRP polymers which take the brittle failure mode if it reaches its ultimate capacity.

2- Increasing the concrete compressive strength in the order of 30 MPa to 60 MPa tends to reduce in the crack width by 54.0 %, while the crack width tends to decrease by 47.0%

when the concrete increasing the concrete compressive strength in the order of 30 MPa to 60 MPa tends to reduce in the crack width by 46 %.

3- The loads deflection curves were semi bilinear for all BFRP reinforced beams. The first part of the curve up to cracking represents the behavior of the un-cracked beams. The second part represents the behavior of the cracked beams with reduced stiffness.

4- The ductility of the group of concrete strength of 30.0 MPa, the ductility ratio was 6.5 % to 10.0 %. For specimens of the second group, the ductility was vary between 6.0 % to 12.0 %. So, using BFRP bars in high strength concrete remain with larger ductility with respect to the specimens with concrete strength 30 MPa. Regardless, the ductility of specimens reinforced with steel bars maintain high ductility.

5- The failure load increased in case of using BFRP bars, regardless the concrete strength as shown in table 4.5 with an average enhancement of 93.0% for specimens of concrete strength of 30.0 MPa. For second group beams the average enhancement in failure load was 93.0%.

6- The cracks were decreased in length and width due to use of BFRP bars as shown in Fig. 14.

References

[1] ACI. Guide for the design and construction of structural concrete reinforced with FRP bars. ACI 440.1R-06, American Concrete Institute, 2006.

[2] Schöck Bauteile GmbH. Germany. March 2015 http://www.schoeck-combar.com/

[3] Polprek Sp. z o.o. Poland. March 2015. http://www.polprek.pl/start

[4] Garbacz A, Łapko A, Urbański M. Investigation on concrete beams reinforced with basalt rebars as an effective alternative of conventional R/C structures. Proceedings of the 11th International Conference on Modern Building Materials, Structures and Techniques. Procedia Engineering 2013; 57:1183-1191.

[5] Baorong Huo. Theoretical and Experimental Study on BFRP Concrete Structure [D]. Doctor Paper of Liaoning Technical University, 2011:29-43.

[6] Kelley L, Michal L. Design philosophy for structural strengthening with FRP [J]. Concrete International, 2000, (2):77-82.

[7] El-Nemr Amr, Ahmed Ehab A, Benmokrane B. Flexural behavior and serviceability of normal- and high-strength concrete beams reinforced with glass fiber-reinforced polymer bars. ACI Struct J 2013;110(6).

[8] Jason Duic, Sara Kenno and Sreekanta Das, “Performance of concrete beams reinforced with basalt fibre composite rebar”, Construction and Building Materials, Vol. 176 (2018), PP. 470–481.

[9] El-Sayed, Taha A., Flexural behavior of RC beams containing recycled industrial wastes as steel fibers. Construction and Building Materials 212, (2019): 27-38.

[10] ANSYS," Engineering Analysis system user's Manual" 2005, vol. 1&2, and theoretical manual. Revision 8.0, Swanson analysis system inc., Houston, Pennsylvania.